Volume 1 | Number 1 | Jan 2013 | Pages 1–100

Molecular Biosystems

www.rsc.org/molecularbiosystems

THE BIOLOGY OF PLAGUE

ROYAL SOCIETY OF CHEMISTRY

ROYAL SOCIETY OF CHEMISTRY

www.rsc.org/molecularbiosystems

1   # ^{1}H NMR brain metabonomics of scrapie exposed

2   # sheep

3

4

5   Paola Scano[1]*, Antonella Rosa[2], Alessandra Incani[2], Caterina Maestrale[3], Cinzia Santucciu[3],

6   Daniela Perra[2], Sarah Vascellari[2], Alessandra Pani[2], Ciriaco Ligios[3]

7

8

9

10   [1] Department of Chemical and Geological Sciences, University of Cagliari, Monserrato, Italy

11   [2] Department of Biomedical Sciences, University of Cagliari, Monserrato, Italy

12   [3] Istituto Zooprofilattico Sperimentale della Sardegna, Sassari, Italy

13

14

16

17
18   * Corresponding author

19   E-mail: scano@unica.it

Abstract

While neurochemical metabolite modifications, found by different techniques, have been diffusely reported in human and mice brains affected by Transmissible Spongiform Encephalopathies (TSEs), this aspect has been little studied in the natural animal host with the same pathological condition so far. Herein, we investigated, by High Resolution ^{1}H NMR spectroscopy and Multivariate Statistical data Analysis, the brain metabolite profile of sheep exposed to scrapie agent in a naturally affected flock. On the basis of clinical examinations and Western Blotting analysis for pathological prion protein (PrP^{Sc}) in brain tissues, sheep were catalogued as not infected (H), infected with clinical signs (S), and infected without clinical signs (A). By discriminant analysis of spectral data, comparing S *vs* H, we found a different metabolite distribution, with inosine, cytosine, creatine, and lactate being higher in S than in H brains, while the branched chain amino acids (leucine, isoleucine, valine), phenylalanine, uracil, tyrosine, gamma-amino butyric acid, total aspartate (aspartate + N-acetyl aspartate) being lower in S. By a soft independent modelling of class analogy approach, 1 out of 3 A samples was assigned to H class. Furthermore, A brains were found to be higher in choline and choline-containing compounds. By means of Partial Least Squares regression, an excellent correlation was found between PrP^{Sc} amount and ^{1}H NMR metabolite profile of infected (S and A) sheep, the metabolite mostly correlated with PrP^{Sc} was alanine. The overall results, obtained by different chemometric tools, were able to describe a brain metabolite profile of infected sheep with and without clinical sign, compared to healthy ones, and indicated alanine as a biomarker for PrP^{Sc} amounts in scrapie brains.

41

Introduction

43   Scrapie is a fatal neurodegenerative disease that affect sheep and goats. This disease belongs to the

44   Transmissible Spongiform Encephalopathies (TSEs), or prion diseases, a group of pathologic

45   conditions that includes bovine spongiform encephalopathy (BSE) of cattle, chronic wasting disease

46   (CWD) of deer, Creutzfeldt-Jakob disease (CJD), and variant CJD (vCJD) in man [1]. TSEs consist

47   in the deposition, within the central nervous system (CNS) and in a number of peripheral nervous

48   and lymphoid tissue districts, of the pathological isoform (PrP^{Sc}) of a normal host protein ("*prion*

49   *protein*", PrP^c) [1]. Studies in rodent models and field observations in sheep suggested that the

50   classical scrapie agent enters into the host's body through the mucosa of the ileal tract of the gut,

51   with the first PrP^{Sc} deposition being observed in Peyer's patches (PPs) and then in other districts of

52   the lymphoreticular system (LRS) [2]. From the LRS, prions enter inside the CNS through the

53   sympathetic and parasympathetic fibers of the autonomic nervous system, with the first appearance

54   of PrP^{Sc} deposition at the level of the *nucleus parasympathicus nervi vagi* (NPNV) and the

55   intermedio-lateral (IML) cell column of the thoracic spinal cord [3]. During the lymphoid spreading

56   of PrP^{Sc} and its early phase of neurodeposition, sheep appear clinically healthy. Following a 2

57   years-long incubation time, onset of clinical scrapie is associated with diffuse PrP^{Sc} deposition,

58   neuronal vacuolation, astrocytosis and microglia activation in the CNS [1]. All these changes result

59   in complex alterations of cellular metabolites that have been studied by means of low resolution

60   Magnetic Resonance Spectroscopy (MRS) *in vivo* and *ex vivo* brains and tissues and by High

61   Resolution Proton Nuclear Magnetic Resonance (^{1}H NMR) in brain extracts [4-6]. In our previous

62   work, analyzing by different techniques lipid composition in brain extracts from healthy and

63   naturally scrapie infected sheep it was observed a significant enrichment in symptomatic- sheep

64   brain of saturated fatty acids, which may affect thermodynamic properties and phase behavior of

65   neuronal membranes [7].

66   "Metabonomics" has been defined as the "understanding the metabolic responses of living

67   systems to pathophysiological stimuli *via* multivariate statistical analysis (MVA) of biological

68   NMR spectroscopic data" [8]. MVA is a powerful tool that allows to extract qualitative and

69   quantitative information from large data sets. Among MVA, qualitative techniques as cluster

70   analysis, principal components analysis (PCA), soft independent modelling of class analogy

71   (SIMCA) are aimed at find similarities and dissimilarities among samples. For sample classification

72   and biomarker identification, discriminant analysis (DA) are more appropriate. Among regression

73   techniques, Partial Least Squares (PLS) can be used to linearly correlate multivariate data with

74   measured response. Multivariate statistical approaches, differently from univariate tests, taking into

75   account correlations among variables, highlight all the concomitant changes of metabolites, thus

76   giving a more ample picture of biomarker candidates and a more robust classification.

77   In this work, in the attempt to identify a metabolite profile linked to prion ailments, we

78   studied, by means of ^{1}H NMR spectroscopy coupled with different MVA, the pool of hydro-soluble

79   low molecular weight compounds in brain extracts from Sarda breed sheep exposed to scrapie agent

80   in a historically affected flock. To accomplish this goal, brains were collected from healthy (H),

81   scrapie-infected symptomatic (S), and infected asymptomatic (A) sheep. Modifications of brain

82   metabolite profile were correlated with PrP^{Sc} deposition, as measured by WB analysis, in brains of

83   the affected animals.

84

85

Material and Methods

Sheep selection, scrapie diagnosis and brain treatments

A scrapie-affected Sarda sheep flock, located in Sardinia (Italy), was studied. The flock was randomly selected among those with high incidence of clinical scrapie. After notification of clinically suspect cases, inside the context of passive surveillance for scrapie, presence of the disease in the flock was assessed by conventional protocols. In this flock, inside the framework of appropriate actions for eradicating scrapie, all the susceptible animals, with or without clinical signs, were euthanized. Whole brains were removed by standard necropsy procedures as soon after death as possible. Collected brains were divided into two hemi-parts by a medial cutting before being frozen at $-80\circ$C. One half underwent Western Blotting (WB) examination [9] and PrP^{Sc} relative quantification. Eighteen brains were selected, based on WB results they were classified as follows: n=7, PrP^{Sc} negative, as healthy (H-1 to H-7); among 11 PrP^{Sc} positive, when clinical signs were previously reported they were classified as symptomatic (n= 8, from S-1 to S-8), otherwise asymptomatic (n=3, from A-1 to A-3). The second half brain was weighed and immediately homogenized in ice for 2 min in saline solution, 1:1 weight:volume, using an Ultra Turrax blender. Aliquots of homogenates were stored at $-80\circ$C.

Extraction of the water-soluble low molecular weight components

For each brain three aliquots were submitted to extraction. The low molecular weight water-soluble components were extracted from homogenized brain samples using a solution of $CHCl_3/MeOH/H_2O$ (2/1/1 v/v/v) according to the Folch method [10]. Briefly, 12 mL of $CHCl_3/MeOH$ were added to brain homogenates (500 mg of wet brain/mL of saline solution). After 1 h, 3 mL H_2O were added in order to solubilize the hydrophilic components. After centrifugation at 900g for 1 h, the $H_2O/MeOH$ mixture, containing the water soluble low molecular weight

109   components, was separated from the $CHCl_3$ phase, that contains the lipid fraction. The water soluble

110   phase (4 mL) was dried by rotor vacuum and redissolved in 600 μl of D_2O. From each brain, three

111   samples were prepared for NMR analysis.

^{1}H NMR experiments

113   ^{1}H NMR spectra were recorded at 499.839 MHz, using a Varian UNITY INOVA 500 spectrometer

114   (Agilent Technologies, CA, USA). Experiments were carried out at 300K, with an acquisition time

115   of 3 s, 20 s relaxation delay, a 90° pulse, and 128 scans. For suppression of residual water

116   resonance, the 1-D NOESY pulse sequence with a mixing time of 1 ms was applied. To the free

117   induction decays (FID) a zero-filling to 128K and a line broadening of 0.3 Hz were applied.

118   Chemical shifts were referred to the resonance of the standard sodium 3-trimethylsilyl-propionate-

119   2,2,3,3,-d_4 (TSP) set at 0.00 ppm. Tentative assignment of signals to metabolites was based on data

120   reported in the literature [11-14], and with the aid of 2D NMR experiments. FID processing, manual

121   phasing, baseline correction and area integration were performed using MestReNova program

122   (Version 7.1.2. Mestrelab Research S.L.).

Data pre-treatment and multivariate statistical data analysis

124   Spectral data pre-treatments were performed to make the samples comparable and the overall data

125   suitable for statistical analysis. To overcome dilution problems, within each sample the integrated

126   area of the spectral regions of interest was reported as percentage of the total integrated areas. The

127   resulting data matrix **X**, in which the rows are samples and columns the spectral integral values (as

128   mean over three spectra from as many as extracts for each brain) was imported into the SIMCA-P+

129   program (Version 13.0, Umetrics, Sweden), and mean centered and scaled to unit variance, column

130   wise. When distribution of a variable presented Skewness, column wise, it was log-transformed.

131   The multivariate statistical approaches for data analysis here employed were: (i) the unsupervised

132   PCA for sample distribution overview, where information regarding class membership are not

133   given. PCA results were graphically reported in the score plots where samples are projected in the

134   multivariate space; (ii) the supervised Partial Least Square - Discriminant Analysis (PLS-DA) and

135   its Orthogonal variant (OPLS-DA) for classification and identification of the most discriminant

136   variables that characterize classes. In the 2-classes OPLS-DA, the between classes variance is

137   expressed in the first component, further orthogonal components are irrelevant to the

138   discrimination, this is of particular interest when a high intra-class variability exist [15]. PLS-DA

139   model quality was evaluated on the basis of the parameters R^2Y (goodness of fit) and Q^2Y

140   (goodness of prediction, determined through cross validation), and tested for overfitting by

141   permutation test (n=400), as implemented in the SIMCA program. Results of two OPLS-DA

142   models can be depicted in the SUS-plot (Shared and Unique Structures–plot), this is a 2D scatter

143   plot of the loading correlation vectors of the predictive components of the two separate models [16];

144   (iii) the supervised classification technique Soft Independent Modelling of Class Analogy (SIMCA)

145   to classify samples as belonging to an already given class, for which they show the largest

146   similarity. In contrast to other supervised pattern recognition techniques (PLS-DA for example),

147   SIMCA is a more versatile approach (soft modeling) which allows the classification of a sample in

148   one or more classes, or in none of them, while discriminant techniques (hard modelling) only allows

149   to classify a sample in a single class. In SIMCA, for each class of samples a PCA is performed,

150   where the appropriate number Principal Components (PCs) to be included is based on the cross-

151   validation procedure, in fact, although the variance explained by the PCA model (R^2X) increases

152   with additional PCs, the analogous in cross-validation, expressed by Q^2X, does not continuously

153   increase with incremental PCs, indicating, at a certain point, that the addition of more PCs into the

154   model will only add noise. SIMCA results were plotted as Cooman's plot, it provides the

155   orthogonal distance from samples to be classified to two selected PCA classes. The critical cut-off

156   class membership limits are also reported, they define distance of samples from each PCA class

157   model, if a sample belongs to a predefined class it should lie within its boundaries. PLS regression

158   is used to find linear relations between a set of independent variables (**X**) and a measured variable

159   (**y**). This technique uses measured properties, to construct models, often based on minimal

160 differences between similar samples, that seek regularities in variable changes linked to the

161 measured property under study. The orthogonal variation of PLS (OPLS) separates the systematic

162 variation in X into two parts, one part that is correlated (predictive) to **y** and the other is

163 uncorrelated (orthogonal) to **y**. [17].

164 PrP^{Sc} quantification in brain

165 To determine the relative amount of PrP^{Sc} / μg in the whole brain of asymptomatic and clinically

166 scrapie sick sheep, we compared the intensity of the WB signals of each brain to a standard curve

167 generated from WB signals of serial naturally-scrapie-infected brain dilutions. To this purpose we

168 used a WB procedure in which the quantification of the total loaded brain proteins was performed

169 with the BCA Protein Assay Kit (23-225 BCA^{TM} Protein Assay Kit, Pierce) and the intensity of the

170 WB signals of the typical PrP^{Sc} bands were captured and quantified by densiometric analysis using

171 a Chemidoc Imager System (BioRad) [18].

172 Ethics statement

173 The protocol used for the slaughtering procedures involving the sheep investigated herein was

174 officially approved by the Service for Animal Welfare of the Istituto Zooprofilattico Sperimentale

175 della Sardegna according to the guidelines n. I 09 044, in tight agreement with the guidelines of

176 Italian National Law n. 116/1992. Sheep were humanely euthanized with a barbituate solution,

177 followed by injection of 4 ml of embutramide and mebenzonic-iodide (Hoechst Roussel Vet, Italy).

178 We declare that the study was carried out on private animals under the request of the owners and all

179 sheep were institutionally examined in the framework of the scrapie surveillance plan, thereby no

180 permission from an ethics committee was needed. The Istituto Zooprofilattico Sperimentale della

181 Sardegna has been commissioned by Italian Health Ministry to carry out all the analysis related to

182 the regional scrapie surveillance plan.

183

184

Results

^{1}H NMR experiments

187   The ^{1}H NMR technique was applied to study the brain metabolite profile of infected and healthy

188   sheep. The ^{1}H NMR spectra of the aqueous phase of brain extracts are characterized by sharp peaks

189   assigned to functional groups of low molecular weight metabolites found in a free state. A

190   representative ^{1}H NMR spectrum of brain extract is shown in Fig. 1, where it has been divided in

191   two main spectral regions having different intensities. The first, Fig. 1A, from 0.5 to 5.0 ppm,

192   contains signals from the aliphatic groups of free amino acids and derivatives, including the three

193   branched chain amino acids (BCAA: valine, leucine, isoleucine), glutamine (Gln), alanine (Ala),

194   aspartate (Asp), N-acetyl aspartate (NAA), gamma-aminobutyric acid (GABA), taurine (Tau);

195   signals of organic acids such as lactate (Lac) and acetate (Ace), the trimethylamine group of choline

196   and choline-containing compounds: 3-glycero-phosphocholine/phosphocoline (Chol), *myo*-inositol

197   (MI), and creatine (Crt). In the spectral portion between 5.5 and 9.0 ppm, Fig. 1B, resonate less

198   intense signals, attributed to the aromatic protons of amino acids such as tyrosine (Tyr),

199   phenylalanine (Phe), and of nucleosides and nucleobases such as uracil (Ura), cytosine (Cyt),

200   inosine (Ino), and hypoxanthine (Hyp); of nicotinammide adenin dinucleotide (NAD), formate

201   (Form) and fumarate (Fum). Other detected NMR peaks were not unambiguously identified, also

202   due to the possible loss of information, linked to ^{2}H exchange of labile protons [19]. Once the

203   spectra were fully assigned, those areas representative of the most relevant metabolites were

204   measured by means of spectral area integration. Being in the intrinsic nature of ^{1}H NMR

205   spectroscopy to detect, in principle, all hydrogens in a molecule, excluding the fast changing ones,

206   several metabolites, such as MI, exhibit resonances in different regions of the spectrum, taking into

207   consideration this observation, areas to be integrated, diagnostic of a single metabolite, were

208   carefully chosen among those being not overlapped and baseline well resolved. Results are reported

209   in Table 1. Seldom, when the 3 different extracts of the same brain were examined, quantitative

210   differences of NAA and its hydrolysis products: N-Ace (N-acetyl) and Asp were observed.

211   Quantitative analysis of the 3 compounds indicated that, to a certain extent, hydrolysis of NAA has

212   taken place [20-21] during sample handling. Considering the reported relevance of NAA in brain

213   diseases [5, 22] to do not lose these information and to, on the other hand, overcome this bias, these

214   molecular components were considered as an unique variable, therefore NAA (2.67 – 2.65 ppm)

215   and Asp (2.83 – 2.76 ppm) normalized integrals were summed up and the new variable was named

216   Asp-tot; analogously, Ace-tot was obtained by summing up N-Ace (singlet at 2.01 ppm) and Ace

217   (singlet at 1.91 ppm) integrals. Following these procedures for each brain a total of 24 variables

218   (reported as means over 3 extracts) ready for MVA were obtained.

219

Data set overview by PCA

221   At a glance, no spectral differences were detectable between the ^{1}H NMR spectra of healthy and

222   infected symptomatic as well as asymptomatic brain extracts. To extract the information, in terms of

223   similarities and dissimilarities of samples based on metabolite characteristics, contained in the set of

224   spectra, a PCA of the spectral data (20 samples and 24 variables) was performed. The first two PCs

225   described 59% of the variance and no outliers were detected. From the analysis of the score plot

226   PC1 *vs* PC2, shown in Fig. 2, it can be seen that S samples lie, although scattered in two groups, in

227   the left side of the plot, while H and A samples, that tend to cluster, are projected in the right side.

228   The results of this unsupervised analysis showed that the healthy and infected brains had different

229   metabolite profiles, and that A brain samples shared common features with the H ones.

230

Discriminant analysis for metabolite identification of H *vs* S samples

232   The results of the PCA showed that the H and S samples had different metabolite profiles and that

233   the S samples presented a higher intra-class variability. To find those metabolites that discriminate

234   the different classes of samples an OPLS-DA was performed on 2 sample classes, H *vs* S. This

235   produced a 2 components validated model with $R^2Y = 0.94$ and $Q^2 = 0.89$, indicating a good fitting

236   and a good classification power. Loading values along the predictive component were studied to

237   attribute discriminant metabolites to each class. Results are reported in Table 2, where only the

238   most important metabolites, i.e. those having the highest loading values that indicate a higher

239   importance (weight) of the variable in discriminating sample class, are reported. The most

240   discriminant variables were found to be Ino, Cyt, Crt, and Lac, up regulated in S samples, while

241   Asp-tot, GABA, Tyr, Ura, Phe, and BCAA were down-regulated.

242

Characterization of A samples

244   The PCA score plot of Fig. 2 showed that H and A samples clustered. To deeper investigate the

245   characteristics of A samples, although numerically very limited, we performed further MVA.

246   SIMCA was used for predicting class belonging of A samples with regard to H and S classes and

247   results visualized in the Cooman's plot reported in Fig. 3, where the multivariate spaces pertinent to

248   H and S classes are shown. This showed that all the S and H samples were placed in their class

249   membership zone. One (A10) out of the 3 infected asymptomatic samples projected into this space,

250   was classified as healthy, while the remaining 2, as not lying within the boundaries of any of the 2

251   (H and S) predefined classes, were classified to neither of the 2 classes.

252   With the aim of finding those metabolites that characterize the A class of samples we performed

253   and cross-compared results of two pair wise OPLS-DA models: "H *vs* A", and "H *vs* S", that were

254   satisfactorily validated ($R^2Y = 0.97$ and $Q^2Y = 0.62$; $R^2Y = 0.94$ and $Q^2Y = 0.89$, respectively). The

255   results, in terms of loading values, are showed as SUS-plot (Fig. 4). It is clearly visible that Chol

256   was the variable that mostly characterized the A samples. It is worth reminding that Chol variable

257   comprises metabolites predominantly involved in choline phospholipid metabolism (choline,

258   phosphocholine and glycerol phosphocholine) [12]. The two classes of infected samples (S and A)

259   shared the metabolite Ino. Metabolites up-regulated in A samples are reported in Table 2.

260

PrP^{sc} amounts and correlation with spectral data by PLS regression

262 The WB analysis, applied to the brain samples of infected symptomatic and asymptomatic sheep,

263 revealed the same PrP^{Sc} molecular signature, thus suggesting that the same scrapie agent was

264 involved in all the examined affected sheep. PrP^{Sc} deposition was demonstrated in all the examined

265 brains of S and A sheep and data reported in Table 3 and (Fig. 5). The PrP^{Sc} amounts were

266 generally higher in the S sheep compared to those in A sheep although Student's *t* test indicated that

267 means are not statistically different. To ascertain whether the metabolite profile of brains is linked

268 to PrP^{sc} quantities, we performed an OPLS regression on NMR data with PrP^{sc} amount as response.

269 Quality of the OPLS regression model was high satisfactory (1+2 components, R^2Y=0.997 and

270 Q^2Y=0.87), thus indicating that there were modifications in the metabolite profile strongly linearly

271 linked to PrP^{sc} amounts. In Table 4 we report the metabolites having the strongest (either positive or

272 negative) correlation with PrP^{sc} levels. Result of *t*-test on Ala data of infected and healthy samples

273 reject the null hypothesis at p>0.05.

274

275

Discussion and Conclusions

277 Our results indicated that clinically scrapie affected sheep have different brain metabolite profile

278 compared to healthy ones, while the asymptomatic affected animals, although more similar to the

279 healthy group, have also their own metabolite features. To our knowledge, this is the first

280 metabonomic study performed in naturally infected sheep with scrapie.

281 In this study, although the number the sheep considered is relatively small, assessing the

282 metabolite profile in the whole brain using ^{1}H NMR and different MVA, we found different

283 metabolite profiles in H, S, and A sheep. As results of the OPLS-DA "S *vs* H" and, as shown in the

284 SUS-plot, Ino is the metabolite having relative higher level in the infected sheep (S and A) when

285 compared with the healthy ones. Cyt, Crt, Lac are discriminant of S samples, and as we can see in

286   the SUS-plot, choline and choline containing compounds (phosphocholine and glycerol

287   phosphocholine) characterized the A samples. Healthy brains were characterized by higher relative

288   levels of BCAA, Phe, Ura, Tyr, GABA, and Asp-tot. It is interesting to note that, correlating the

289   metabolite profiles to the PrP^{Sc} amounts, Ala was the most important metabolite, having the

290   strongest positive correlation with PrP^{Sc} amount. GABA, Ura, and Asp-tot were those metabolites

291   that both were inversely correlated with PrP^{Sc} levels and discriminated H samples.

292   We found a higher level of Lac in the extracts of S brains when compared to the H ones. It,

293   generally, indicates a more intense anaerobic metabolism which can be observed under

294   hypoxic/anoxic stress situations affecting the brains or other organs and can indicate ischemic

295   processes and apoptosis. Being not significantly correlated with PrP^{sc} amounts, it can be hypothesize

296   that increase of Lac is a sign of general sickness although not specifically linked to PrP^{sc} generation.

297   Ino was found to be in relatively higher quantity in S and A brains, it is the breakdown product of

298   ATP, it is formed by deamination of adenosine, mainly at high intracellular concentrations, which

299   are associated with hypoxia, ischemia and other forms of cellular stress [22]. Crt is higher in S

300   brains and also correlated with PrP^{sc}. Crt is thought to have a multifaceted role in the brain. Besides

301   being involved in brain osmoregulation, it has recently been implicated in energy homeostasis and

302   direct antioxidant effects [24, 25]. Furthermore, Crt plays an integral role in cellular energy

303   metabolism, and thus an increase in concentration of this compound may be a result of metabolic

304   stress. Dysregulation of Crt may implicate an energetic shift in the brain, suggesting an increased

305   metabolic activity and/or a depletion of energy storage capacity [22, 24]. Crt has several potential

306   neuroprotective effects [25], including buffering intracellular mitochondrial energy reserves,

307   stabilizing intracellular calcium, and inhibiting activation of the mitochondrial permeability

308   transition pore, which have all been linked to apoptotic and oxidative cell death [27]. Asymptomatic

309   samples are characterized by choline, phosphocholine and glycerol phosphocholine. Choline is an

310   essential nutrient with a complex role in the body. It is required for synthesis of the neurotransmitter

311   acetylcholine and of phosphatydilcholine the major constituent of membranes [11]. It is also

312   involved in cell-membrane signaling (phospholipids), lipid transport (lipoproteins), and methyl

313   group metabolism (homocysteine reduction) [28]. In MRS, choline is a marker of cellular

314   membrane turnover, and is therefore elevated in neoplasms, demyelination and

315   gliosis. Phosphocholine, that contributes to the choline resonance, may act as a biomarker for

316   membrane phospholipid metabolism/turn over [29]. Choline is also a constituent of sphingolipids

317   that participate to the formation of the lipid rafts where the GPI protein is anchored. Naslavsky [30]

318   reported that in neuroblastoma cells infected with prions, sphingolipid depletion increases formation

319   of the PrP^{Sc}. Deregulation of sphingolipids metabolism in Alzheimer's disease has also been

320   reported [31]. Choline biomarker in A brains could be an early sign of brain cellular membrane

321   damage due to lipid raft formation and protein anchorage. Amino acids play important function as

322   neurotransmitters providing both excitatory and inhibitory stimuli. Here, we found that the amino

323   acid levels of Asp-tot, Tyr, Phe, BCAA are lower in the brains of S sheep. This may be the

324   consequence of the neurodegenerative phenomena affecting pre- and post-synaptic processes, a

325   commune pattern observed in distinct brain regions when exposed to prion [32] or to beta-amyloid

326   olygomers in Alzheimer's disease. The loss of a selective subpopulation GABAergic neurons has

327   been demonstrated in experimentally prion infected mouse [33] by detecting

328   immunohistochemically the glutamic acid decarboxylase, the GABA synthesizing enzyme. This

329   correlates well with our observation of lower level of GABA in the S brains when compared to H.

330   Moreover, the lower GABA level seems to be relegated to the clinical stage of scrapie, as being not

331   observed as discriminant in the asymptomatic sheep. In this respect, a decrease of the GABA

332   activity has been observed at the clinical stage in scrapie infected hamster [34]. Asp-tot (comprising

333   NAA and Asp) level is lower in S and A sheep. Decrease of NAA is a finding already described

334   also at earlier stages of disease in murine model after experimental prion infection [6]. NAA is an

335   abundant metabolite which is present only in neurones in the adult brain, and although its role in the

336   cell is little know, it is widely considered to be a marker of functional neurons. [6]. A lower level of

337   Ura has been observed in brains of symptomatic sheep when compared to the healthy ones.

338   Although little is known on the neuronal functions of Ura, it has been suggested that it modulates

339   many neurotransmitters or neuromodulators, especially in the mature central nervous system [35]

340   and its glycosylated form, Uridine, has been proposed as neuroprotective agent in

341   neurodegenerative disorders [36]. Ala was the metabolite more strongly linked to PrP^{sc} amount in

342   scrapie sheep brains. Ala has been indicated as a biomarker of apoptosis and/or cellular stress

343   processes in brain, which are both normally observed in scrapie neuropathology [37]. In addition,

344   increase of Ala has been observed also in meningioma and following ischemia [38], as well as

345   concentration of plasma Ala was significantly increased ($P < 0.05$) in infected BSE dairy cattle

346   [39].

347   Among the biases that could affect the reliability of our results, the potential presence of

348   different scrapie agent strains implicated in our cases should be taken into account. In general,

349   neuropathological changes, including PrP^{Sc} molecular signature and its regional distribution in the

350   brain, are strictly related to the TSE agent strain involved and to the PrP genotype of the host, thus

351   these differences related to the host might influence the ^{1}HMRS neuro-metabolic profile [40]. Our

352   study has the advantage that all cases belong to the same flock, and only one identical molecular

353   signature was found among the different examined cases. In addition, it is worth to recall that only

354   one identical scrapie agent strain has been found in Italy so far [41].

355   The approach here described was able to identify different metabolite profiles pertaining to

356   healthy and infected sheep brains, physiopathological roles of metabolites mainly involved may

357   explain their different expression in these two extreme situations. Determining the metabolite

358   modifications in the asymptomatic and symptomatic phases of the disease might clarify some of the

359   molecular mechanisms of the prion disease and disease progression. As in previous studies, our

360   findings confirm the close relationship between scrapie and other neurodegenerative diseases,

361   although to compare ruminant brain metabolites to human's can be, to some extent, hazardous. This

362   study concerns *in vitro* analysis of the whole brain, whereas the pathology onset e widespread has

363 specific neuroanatomical locations, in this respect, future investigations will be dedicated to the

364 study of metabolite fingerprint in different affected areas.

365 ## Acknowledgement

371

372 ## Funding

375

376

377 # References

378 1. Prusiner SB (1998) Prions. Proc Natl Acad Sci USA 95: 13363-13383.

379 2. Andréoletti O, Berthon P, Marc D, Sarradin P, Grosclaude J, van Keulen L, Schelcher F, Elsen
380   JM, Lantier F (2000) Early accumulation of PrPSc in gut-associated lymphoid and nervous
381   tissues of susceptible sheep from a Romanov flock with natural scrapie. J Gen Virol. 81: 3115–
382   3126.

383 3. van Keulen LJ, Schreuder BE, Vromans ME, Langeveld JP, Smits MA (2000) Pathogenesis of
384   natural scrapie in sheep. Arch Virol Suppl. 16: 57-71.

385 4. Tsang TM, Woodman B, McLoughlin GA, Griffin JL, Tabrizi SJ, Bates GP, Holmes E (2006)
386   Metabolic characterization of the R6/2 transgenic mouse model of Huntington's disease by high-
387   resolution MAS ^{1}H NMR spectroscopy. J Proteome Res. 5: 483-92.

388 5. Holmes E, Tsang T M, Tabrizi SJ (2006) The application of NMR-based metabonomics in
389   neurological disorders. *NeuroRx, 3:* 358-372.

390 6. Broom KA, Anthony DC, Lowe JP, Griffin JL, Scott H, Blamire AM, Styles P, Perry VH,
391   Sibson NR (2007) MRI and MRS alterations in the preclinical phase of murine prion disease:
392   association with neuropathological and behavioural changes. Neurobiol Dis. 26:707-17.

393 7. Rosa A, Scano P, Incani A, Pilla F, Maestrale C, Manca M, Ligios C, Pani A (2013) Lipid
394   profiles in brains from sheep with natural scrapie. *Chemistry and physics of lipids*, 175, 33-40.

395 8. Nicholson JK, Lindon JC, Holmes E. (1999) 'Metabonomics': understanding the metabolic
396   responses of living systems to pathophysiological stimuli via multivariate statistical analysis of
397   biological NMR spectroscopic data. Xenobiotica 29: 1181-9.

398 9. Ligios C, Cancedda MG, Madau L, Santucciu C, Maestrale C, Agrimi U, Ru G, DiGuardo G
399   (2006). PrP[(Sc)] deposition in nervous tissues without lymphoid tissue involvement is frequently
400   found in ARQ/ARQ Sarda breed sheep preclinically affected with natural scrapie. Arch. Virol.
401   151: 2007–2020.

402 10. Folch J, Lees M, Sloane-Stanley GH (1957) A simple method for the isolation and
403   purification of total lipid from animals tissues. J. Biol. Chem. 226,497–509.

404 11. Govindaraju V, Young K, Maudsley AA (2000) Proton NMR chemical shifts and coupling
405   constants for brain metabolites. NMR Biomed. 13: 129–153.

406 12. Viola A, Saywell V, Villard L, Cozzone PJ, & Lutz NW (2007) Metabolic fingerprints of
407   altered brain growth, osmoregulation and neurotransmission in a Rett syndrome model. PLoS
408   One, 2(1), e157.

409   13.   Wishart DS, Knox C, Guo AC, Eisner R, Young N, Gautam B, Hau DD, Psychogios N,

410   Dong E, Bouatra S, Mandal R, Sinelnikov I, Xia J, Jia L, Cruz JA, Lim E, Sobsey CA,

411   Shrivastava S, Huang P, Liu P, Fang L, Peng J, Fradette R, Cheng D, Tzur D, Clements M,

412   Lewis A, De Souza A, Zuniga A, Dawe M, Xiong Y, Clive D, Greiner R, Nazyrova A,

413   Shaykhutdinov R, Li L, Vogel HJ, Forsythe I (2009) HMDB: a knowledgebase for the human

414   metabolome. Nucleic Acids Res. 37:603-10.

415   14.   Scano P, Rosa A, Locci E, Manzo G, Dessì MA (2012) Modifications of the ^{1}H NMR

416   metabolite profile of processed mullet (*Mugil cephalus*) roes under different storage

417   conditions. Magnetic Resonance in Chemistry, 50; 436-442.

418   15.   Bylesjö M, Rantalainen M, Cloarec O, Nicholson JK, Holmes E, Trygg J (2006) OPLS

419   discriminant analysis: combining the strengths of PLS-DA and SIMCA classification. Journal of

420   Chemometrics, 20:341-351.

421   16.   Wiklund S, Johansson E, Sjöström L, Mellerowicz EJ, Edlund U, Shockcor JP, Gottfries J,

422   Moritz T, and Trygg J (2008) Visualization of GC/TOF-MS-Based Metabolomics Data for

423   Identification of Biochemically Interesting Compounds Using OPLS Class Models. Anal. Chem.

424   80:115-122.

425   17.   Eriksson L, Johansson E, Kettaneh-Wold N, Trygg J, Wikstrom C, Wold S (2013) Multi-and

426   Megavariate Data Analysis, 3rd edition; Umetrics Academy, Sweden.

427   18.   Ligios C, Cancedda GM, Margalith I, Santucciu C, Madau L, Maestrale C, Basagni M, Saba

428   M, Heikenwalder M. (2007) Intraepithelial and interstitial deposition of pathological prion

429   protein in kidneys of scrapie-affected sheep. PLoS One 12;2(9):e859.

430   19.   Commodari F, Arnold DL, Sanctuary BC, Shoubridge EA (1991) ^{1}H NMR characterization

431   of normal human cerebrospinal fluid and the detection of methylmalonic acid in a vitamin B12

432   deficient patient. NMR in biomedicine, 4:192-200.

433   20.   Ratai, E. M., Pilkenton, S., Lentz, M. R., Greco, J. B., Fuller, R. A., Kim, J. P., He, J.,

434   Cheng, L. L. and González, R. G. (2005), Comparisons of brain metabolites observed by

435   HRMAS ^{1}H NMR of intact tissue and solution ^{1}H NMR of tissue extracts in SIV-infected

436   macaques. NMR Biomed., 18: 242–251. doi: 10.1002/nbm.953.

437   21.   Moffett JR, Arun P, Ariyannur PS, & Namboodiri AM (2013) N-Acetylaspartate reductions

438   in brain injury: impact on post-injury neuroenergetics, lipid synthesis, and protein

439   acetylation. *Frontiers in neuroenergetics*, *5*.

440   22.   Baslow MH (2003) N-acetylaspartate in the vertebrate brain: metabolism and

441   function. Neurochemical research, 28: 941-953.

442 23. Haskó G, Sitkovsky MV, Szabo C (2004) Immunomodulatory and neuroprotective effects of
443 inosine. *Trends in pharmacological sciences*, *25:* 152-157.

444 24. Pears MR, Cooper JD, Mitchison HM, Mortishire-Smith RJ, Pearce DA, & Griffin JL
445 (2005) High resolution ^{1}H NMR-based metabolomics indicates a neurotransmitter cycling deficit
446 in cerebral tissue from a mouse model of Batten disease. Journal of Biological Chemistry, 280:
447 42508-42514.

448 25. Zhang W, Narayanan M and Friedlander RM (2003) Additive neuroprotective effects of
449 minocycline with creatine in a mouse model of ALS. Ann Neurol., 53: 267–270.
450 doi: 10.1002/ana.10476.

451 26. Lan MJ, McLoughlin GA, Griffin JL, Tsang TM, Huang JTJ, Yuan P, & Bahn S (2008)
452 Metabonomic analysis identifies molecular changes associated with the pathophysiology and
453 drug treatment of bipolar disorder. Molecular psychiatry, 14*:* 269-279.

454 27. Tabrizi SJ, Blamire AM, Manners DN, Rajagopalan B, Styles P, Schapira AH, Warner TT
455 (2003) Creatine therapy for Huntington's disease: clinical and MRS findings in a 1-year pilot
456 study. Neurology, 61(1): 141-2.

457 28. Zeisel SH, Da Costa KA (2009) Choline: an essential nutrient for public health. Nutrition
458 reviews, 67(11), 615-623.

459 29. Senaratne R, Milne AM, MacQueen GM, & Hall GB (2009) Increased choline-containing
460 compounds in the orbitofrontal cortex and hippocampus in euthymic patients with bipolar
461 disorder: a proton magnetic resonance spectroscopy study. Psychiatry Research:
462 Neuroimaging, 172: 205-209.

463 30. Naslavsky N, Shmeeda H, Friedlander G, Yanai A, Futerman AH, Barenholz Y, Taraboulos
464 A (1999) Sphingolipid depletion increases formation of the scrapie prion protein in
465 neuroblastoma cells infected with prions. *Journal of Biological Chemistry*, *274*(30), 20763-
466 20771.

467 31. He X, Huang Y, Li B, Gong CX, & Schuchman EH (2010) Deregulation of sphingolipid
468 metabolism in Alzheimer's disease. Neurobiology of aging, 31: 398-408.

469 32. Siskova Z, Reynolds RA, O'Connor V, Perry VH (2013) Brain region specific pre-synaptic
470 and post-synaptic degeneration are early components of neuropathology in prion disease. PLoS
471 ONE 8(1): e55004. doi:10.1371/journal.pone.0055004.

472 33. Guentchev M, Groschup MH, Kordek R, Liberski PP, Budka H (1998) Severe, early and
473 selective loss of a subpopulation of GABAergic inhibitory neurons in experimental transmissible
474 spongiform encephalopathies. Brain Pathol. 8: 615-23.

475   34.   Durand-Gorde JM, Bert J, Nieoullon A (1984) Early changes in tyrosine hydroxylase,
476   glutamic acid decarboxylase and choline acetyltransferase golden hamster striatum after
477   intracerebral inculation of the nigrostriatal system with scrapie agent (263K). Neurosc. Lett. 51:
478   37-42.

479   35.   Lecca D, Ceruti S (2008) Uracil nucleotides: From metabolic intermediates to
480   neuroprotection and neuroinflammation. Biochemical Pharmacology, 75: 1869-1881, ISSN
481   0006-2952, doi:10.1016/j.bcp.2007.12.009.

482   36.   Dobolyi A, Juhasz G, Kovacs Z, Kardos J (2011) Uridine function in the central nervous
483   system. Current topics in medicinal chemistry, 11:1058-1067.

484   37.   Schätzl HM, Laszlo L, Holtzman DM, Tatzelt J, DeArmond SJ, Weiner RI, Mobley WC,
485   Prusiner SB (1997) A hypothalamic neuronal cell line persistently infected with scrapie prions
486   exhibits apoptosis. J Virol. 71: 8821-31.

487   38.   Reinke SN, Walsh BH, Boylan GB, Sykes BD, Kenny LC et al. (2013) ^{1}H NMR derived
488   metabolomic profile of neonatal asphyxia in umbilical cord serum: implications for hypoxic
489   ischemic encephalopathy. Journal of Proteome Research 12: 4230-4239.

490   39.   Allison GG, Horton RA, Rees Stevens P, Jackman R, Moorby JM (2008) Changes in plasma
491   metabolites and muscle glycogen are correlated to bovine spongiform encephalopathy in infected
492   dairy cattle. Research in Veterinary Science, 80:40-46. j.rvsc.2006.11.008.

493   40.   Lodi R, Parchi P, Tonon C, Manners D, Capellari S, Strammiello R, Rinaldi R, Testa C,
494   Malucelli E, Mostacci B, Rizzo G, Pierangeli G, Cortelli P, Montagna P and Barbiroli B (2009)
495   Magnetic resonance diagnostic markers in clinically sporadic prion disease: a combined brain
496   magnetic resonance imaging and spectroscopy study. Brain: 132: 2669–2679.

497   41.   Nonno R, Esposito E, Vaccari G, Conte M, Marcon S, Di Bari M, Ligios C, Di Guardo G,
498   Agrimi U (2003) Molecular analysis of cases of Italian sheep scrapie and comparison with cases
499   of bovine spongiform encephalopathy (BSE) and experimental BSE in sheep. J Clin Microbiol
500   41: 4127–4133.

501

502

503

504 **Table 1. Selected spectral regions and assigned metabolites used for this study.**

Metabolites (abbreviations)	Functional group[a]	multiplicity[b]	range (ppm)[c]
BCAA[d]	$-CH_3$	m	1.06 - 0.89
Alanine (Ala)	$-CH_3$	s	1.49 - 1.46
Acetate (Ace)	$-CH_3$	s	1.91
N-Acetyl groups (N-Ace)	$-CH_3$	s	2.01
GABA	$-\beta CH_3$		2.32 - 2.27
Glutamate (Glu)	$-\gamma CH_2$	m	2.37 - 2.32
Glutamine (Gln)	$-\gamma CH_2$	m	2.48 - 2.42
N-acetyl aspartate (NAA)	$-\beta CH_2$	dd	2.67 – 2.65
Aspartate (Asp)	$-\beta CH_2$	dd	2.83 – 2.76
Choline[e] (Chol)	$-N(CH_3)_3$	s	3.25 - 3.19
Scyllo-inositol (SI)	$-CH$	s	3.37 - 3.33
Taurine (Tau)	$S-CH_2$	t	3.46 - 3.41
Creatine (Crt)	$N-CH_2$	s	3.95 - 3.92
Myo-inositol (MI)	$-C2H$	t	4.09 - 4.04
Lactate (Lac)	$-CH$	q	4.15 - 4.08
Uracil (Ura)	$-C5H$	d	5.83 - 5.79
Nucleosides (Nucl)	$-C3H, -C5H$	d	5.94 - 5.90
Cytosine (Cyt)	$-C5H$	d	6.12 - 6.09
Fumarate (Fum)	$-(CH)_2$	s	6.51
Tyrosine (Tyr)	$-C3H, -C5H$	d	6.92 - 6.88
Phenylalanine (Phe)	$-C3H, -C4H, -C5H, -C6H$	m	7.45 - 7.31
Xanthine (Xan)	$-CH$	s	7.94
Hypoxanthine (Hyp)	$-CH$	s	8.28 - 8.17
Inosine (Ino)	$-CH$	s	8.36
ATP/ADP/AMP (AP)	$-CH$	s	8.45
NAD	$-C6H$	d	8.75 - 8.68
NAD	$-C8H$	s	8.96 - 8.90

505 a) The molecule numbering system follows IUPAC rules; b) s= singlet, d= doublet, t = triplet, m=
506 multiplet; c) ppm with respect to TSP; d) branched chain amino acids; e) choline and choline-
507 containing compounds.

508

509

510 **Table 2. OPLS-DA most discriminant metabolites of S and A classes compared to H class.**

Metabolites	classes	
	S	**A**
Ino[a]	↑[b]	↑
Chol	--	↑
Asp-tot	↓	↓
GABA	↓	↑
Lactate	↑	↑
BCAA	↓	↓
Cyt	↑	--
Phe	↓	--
Tyr	↓	--
Crt	↑	--
Uracil	↓	--
Ala	↑	↑
Fum	--	↓

511 a) Inosine (Ino), choline/phosphocholine/3-glycero-phosphocholine (Chol), aspartate + N-
512 acetylaspartate (Asp-tot), gamma-aminobutyric acid (GABA), lactate (Lac), BCAA (branched chain
513 aminoacids: isoleucine, leucine, and valine), cytosine (Cyt), phenylalanine (Phe), tyrosine (Tyr),
514 creatine (Crt), uracil (Ura), alanine (Ala), fumarate (Fum). b) ↑ up-regulated**,** ↓ down-regulated,
515 and **--** stable, with respect to the H class**.**

516

517

518

519

Table 3. PrP^{Sc} amounts^a, as calculated by WB analysis in brains of infected sheep.

Sample		Density OD/mm^2
Infected symptomatic		
S-1		181.89
S-2		130.02
S-3		223.09
S-4		198.06
S-5		187.92
S-6		176.35
S-7		204.60
S-8		167.03
	Mean	183.62
	SD	27.85
Infected asymptomatic		
A-9		104.26
A-10		171.93
A-11		124.01
	Mean	133.40
	SD	34.79

520   a) means are not statistically different.

521

522

Table 4. OPLS metabolites having the strongest (positive or negative) correlation with PrP^{sc} amounts in brain homogenates.

Metabolites	r^a	R^{2b}	loadings^c	loadings cv^d
Directly correlated ↑				
Ala	0.861	0.742	0.327	0.099
Cyt	0.803	0.645	0.300	0.103
Crt	0.639	0.408	0.248	0.119
Inversely correlated ↓				
Asp-tot	-0.780	0.608	-0.302	0.162
Ura	-0.609	0.370	-0.237	0.183
GABA	-0.602	0.363	-0.218	0.102

a) coefficient of correlation and b) coefficient of determination of metabolite *vs* PrP^{sc} amounts; c) loading weights along the predictive component; d) Jack-knife standard error of loading weights computed from all rounds of cross validation. Alanine (Ala), cytosine (Cyt), creatine (Crt), aspartate + N-acetylaspartate (Asp-tot), uracil (Ura), gamma-aminobutyric acid (GABA).

24

Figure captions

Fig. 1. A representative ^{1}H NMR spectrum of brain extract. (**A**) spectral region from 0.5 to 5.0 ppm and (**B**) spectral region from 5.5 to 9.0 ppm (magnified). Major assignments are reported. Branched chain aminoacids: isoleucine, leucine, and valine (BCAA), lactate (Lac), alanine (Ala), acetate (Ace), N-acetyl groups (N-Ace), gamma-aminobutyric acid (GABA), glutamate/glutamine (Glx), N-Acetylaspartate (NAA), aspartate (Asp), creatine (Crt), choline/phosphocholine/3-glycero-phosphocholine (Chol), taurine (Tau), *myo*-inositol (MI), *scyllo*-inositol (SI), Cytosine (Cyt), Nucleosides (Nucl), Uracil (Ura), Fumarate (Fum), Tyrosine (Tyr), Phenylalanine (Phe), Xanthine (Xan), Hypoxanthine (Hyp), Inosine (Ino), ATP/ADP/AMP (AP), NAD.

Fig. 2. **PCA of brain extracts spectral data.** PCA of ^{1}H NMR spectral data of brain extracts, PC1 *vs* PC2 score plot of S (boxes), H (circles), and A (triangles) samples. The explained variance is reported in brackets. Ellipse encloses the 95% Hotelling T^2 confidence region.

Fig. 3. **Cooman's plot of brain extracts spectral data.** SIMCA Cooman's plot. In the x-axis PCA of H samples: 47% of total variance expressed, 2 components; in the y-axis PCA of S samples: 65% of total variance expressed, 2 components for S. The plot is divided into four regions by the intersection of 95% confidence limit lines for each class. These regions identify the class membership: the NW region defining H only, the SE region defining S only, the SW region containing both H and S, and the NE region containing neither H nor S membership.

Fig. 4. **SUS plot of brain extracts spectral data.** Loading SUS-plot of OPLS-DA models of ^{1}H NMR data of brain extracts. In the x-axis the loading correlation values of "H *vs* A" model and in the y-axis the loading correlation values of "H *vs* S" model. Variables in the lower left corner are unique for H samples, variables in the higher right corner are shared in infected (S and A) samples. Variables higher in S and A samples exhibit high correlation values in the y- and x-axes, respectively. Branched chain aminoacids: isoleucine, leucine, and valine (BCAA), lactate (Lac), alanine (Ala), acetate + N-acetyl groups (Ace-tot), gamma-aminobutyric acid (GABA), glutamate (Glu), glutamine (Gln), aspartate + N-acetylaspartate (Asp-tot), creatine (Crt), choline/phosphocholine (Chol), taurine (Tau), myo-inositol (MI), scyllo-inositol (SI), Cytosine

566   (Cyt), Nucleosides (Nucl), Uracil (Ura), Fumarate (Fum), Tyrosine (Tyr), Phenylalanine (Phe),

567   Xanthine (Xan), Hypoxanthine (Hyp), Inosine (Ino), ATP/ADP/AMP (AP), NAD.

568

569   **Fig. 5. Quantification of PrP^{Sc} in brain homogenates of naturally scrapie-affected sheep. (A)**

570   Western blot (WB) analysis of whole-brain homogenate after proteinase K (PK) digestion from

571   independent symptomatic (lines 2 to 9) and asymptomatic (lines 10 to 13) scrapie affected sheep. A

572   molecular weight marker is loaded in lane 1. (B) Quantification of the WB signal of the PrP^{Sc}

573   present in the brain homogenates is represented as PrP optical density (OD) signals. Our results

574   indicate that the higher average amount of PrP^{Sc} was detected in the symptomatic scrapie affected

575   sheep. The brain homogenate samples were normalized in relation to the total protein amount.
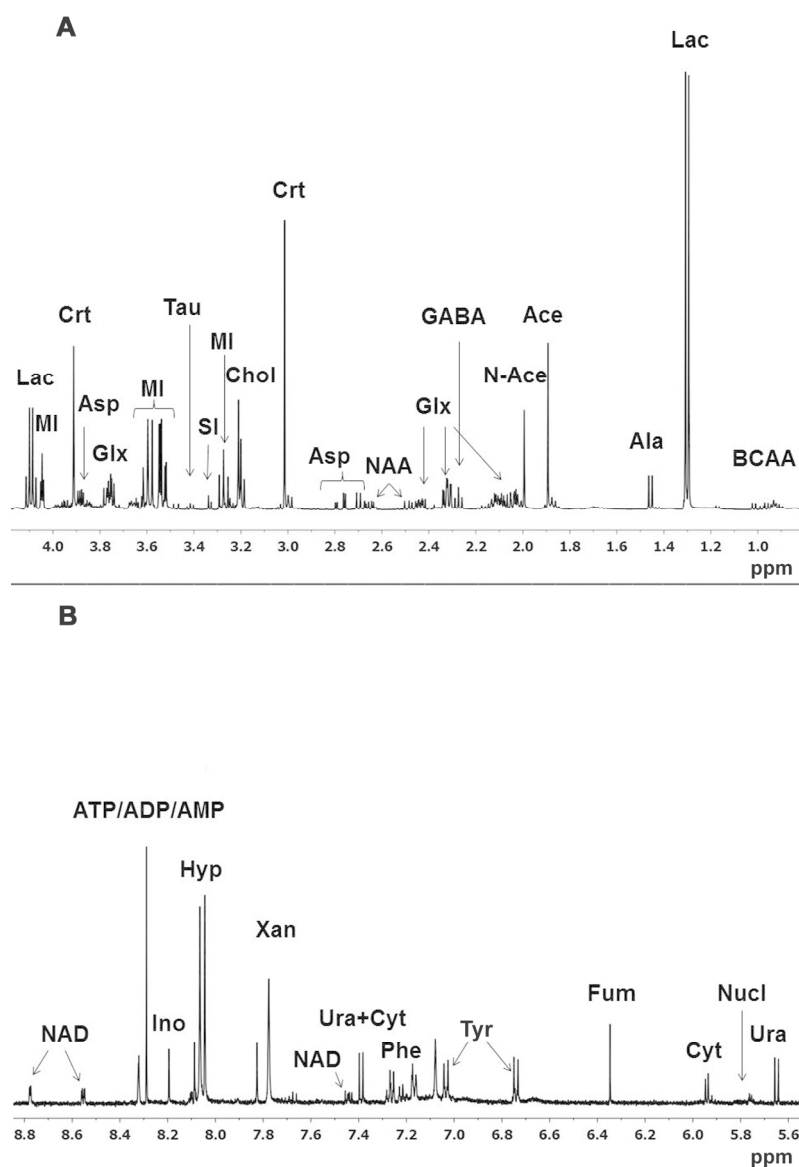
576

577

Fig. 1. A representative ^{1}H NMR spectrum of brain extract. (A) spectral region from 0.5 to 5.0 ppm and (B) spectral region from 5.5 to 9.0 ppm (magnified). Major assignments are reported. Branched chain aminoacids: isoleucine, leucine, and valine (BCAA), lactate (Lac), alanine (Ala), acetate (Ace), N-acetyl groups (N-Ace), gamma-aminobutyric acid (GABA), glutamate/glutamine (Glx), N-Acetylaspartate (NAA), aspartate (Asp), creatine (Crt), choline/phosphocholine/3-glycero-phosphocholine (Chol), taurine (Tau), myo-inositol (MI), scyllo-inositol (SI), Cytosine (Cyt), Nucleosides (Nucl), Uracil (Ura), Fumarate (Fum), Tyrosine (Tyr), Phenylalanine (Phe), Xanthine (Xan), Hypoxanthine (Hyp), Inosine (Ino), ATP/ADP/AMP (AP), NAD.
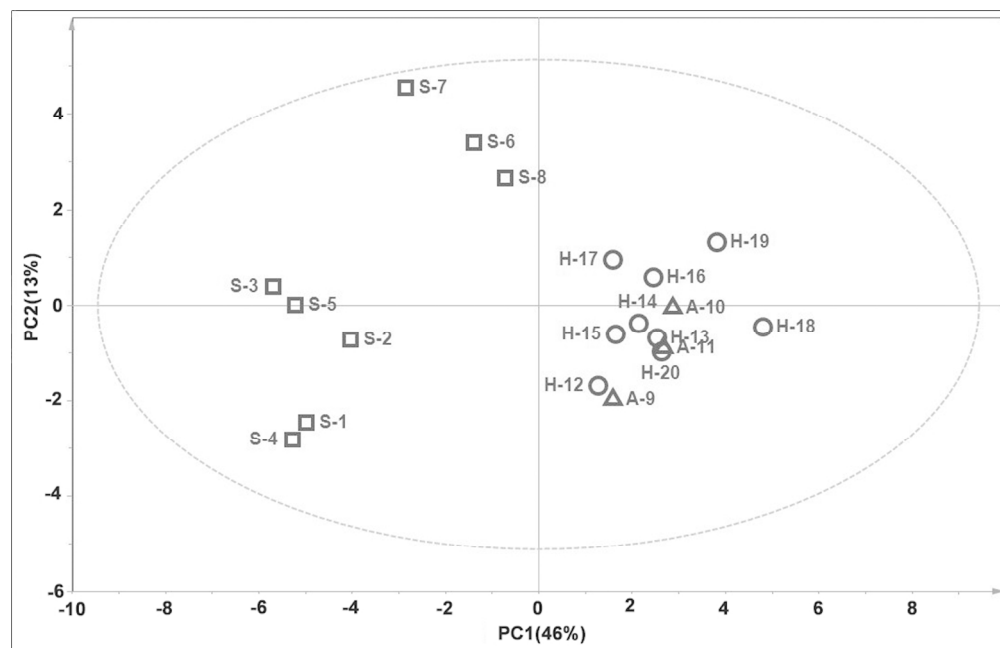
124x189mm (300 x 300 DPI)

Fig. 2. PCA of brain extracts spectral data. PCA of 1H NMR spectral data of brain extracts, PC1 vs PC2 score plot of S (boxes), H (circles), and A (triangles) samples. The explained variance is reported in brackets. Ellipse encloses the 95% Hotelling T2 confidence region.
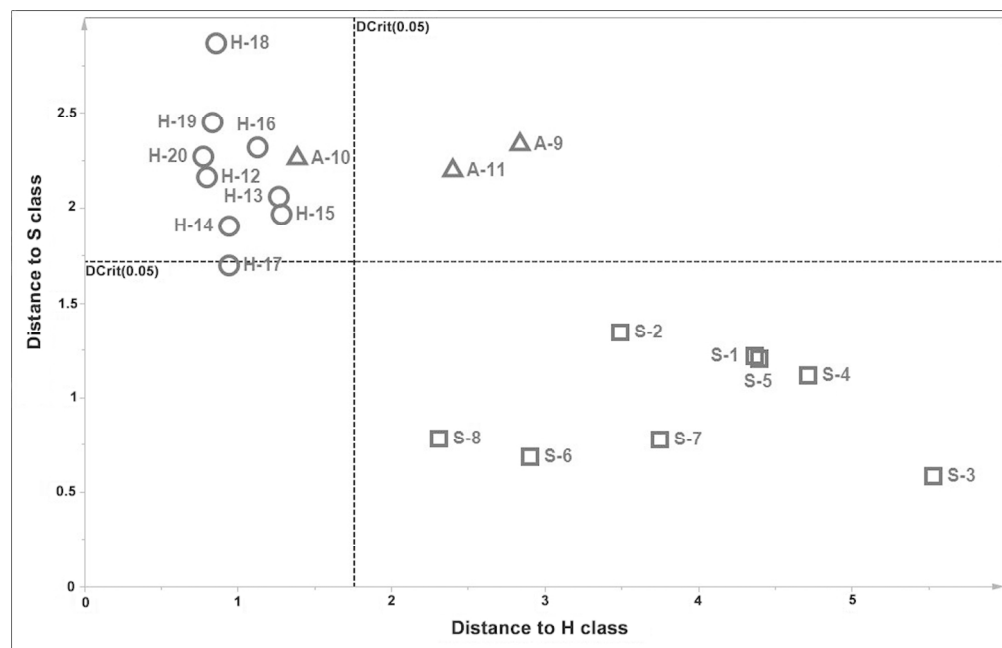124x80mm (300 x 300 DPI)

Fig. 3. Cooman's plot of brain extracts spectral data. SIMCA Cooman's plot. In the x-axis PCA of H samples: 47% of total variance expressed, 2 components; in the y-axis PCA of S samples: 65% of total variance expressed, 2 components for S. The plot is divided into four regions by the intersection of 95% confidence limit lines for each class. These regions identify the class membership: the NW region defining H only, the SE region defining S only, the SW region containing both H and S, and the NE region containing neither H nor S membership.
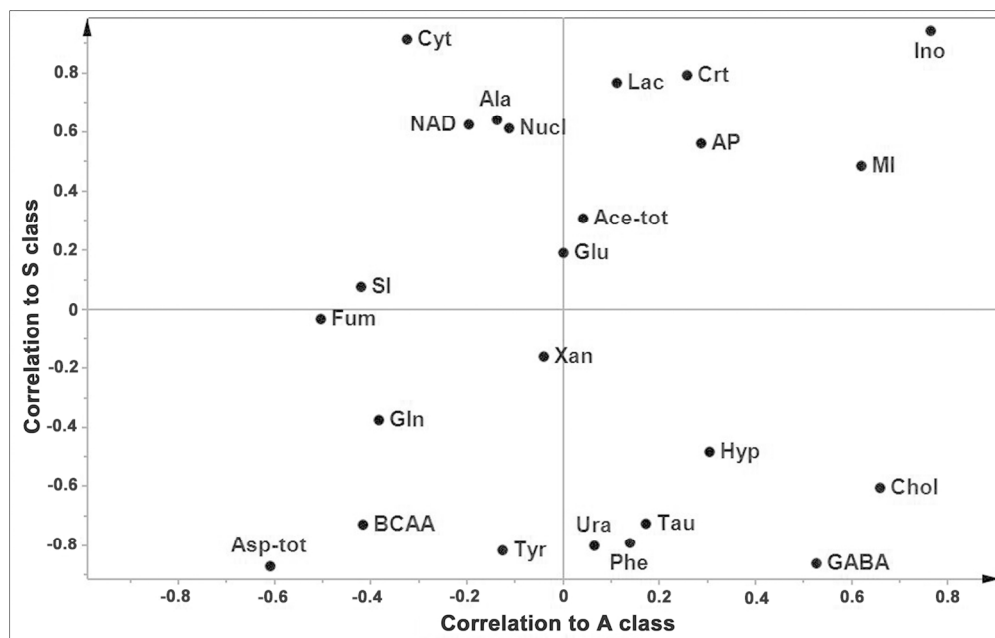
124x80mm (300 x 300 DPI)

Fig. 4. SUS plot of brain extracts spectral data. Loading SUS-plot of OPLS-DA models of 1H NMR data of brain extracts. In the x-axis the loading correlation values of "H vs A" model and in the y-axis the loading correlation values of "H vs S" model. Variables in the lower left corner are unique for H samples, variables in the higher right corner are shared in infected (S and A) samples. Variables higher in S and A samples exhibit high correlation values in the y- and x-axes, respectively. Branched chain aminoacids: isoleucine, leucine, and valine (BCAA), lactate (Lac), alanine (Ala), acetate + N-acetyl groups (Ace-tot), gamma-aminobutyric acid (GABA), glutamate (Glu), glutamine (Gln), aspartate + N-acetylaspartate (Asp-tot), creatine (Crt), choline/phosphocholine (Chol), taurine (Tau), myo-inositol (MI), scyllo-inositol (SI), Cytosine (Cyt), Nucleosides (Nucl), Uracil (Ura), Fumarate (Fum), Tyrosine (Tyr), Phenylalanine (Phe), Xanthine (Xan), Hypoxanthine (Hyp), Inosine (Ino), ATP/ADP/AMP (AP), NAD.
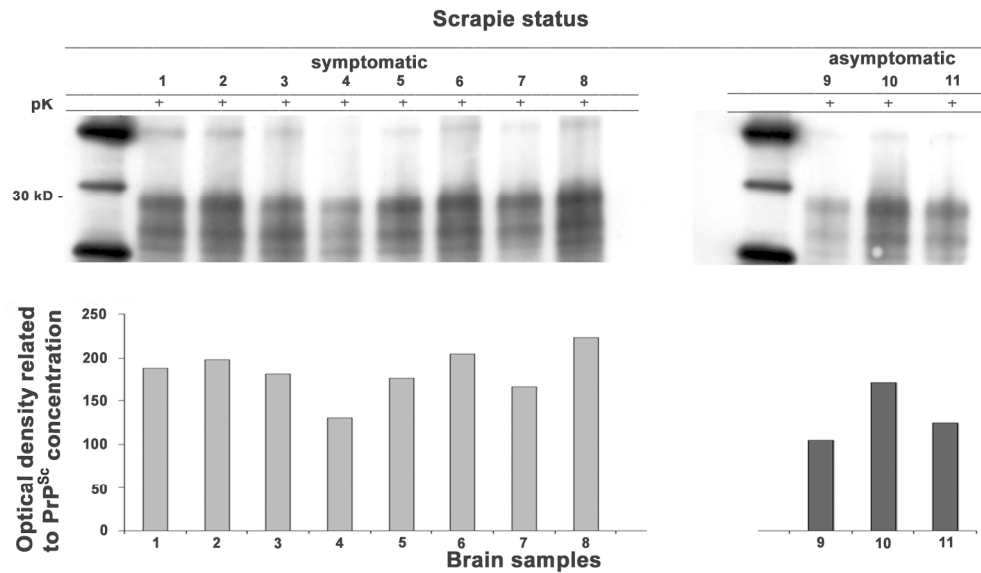124x79mm (300 x 300 DPI)

Fig. 5. Quantification of PrPSc in brain homogenates of naturally scrapie-affected sheep. (A) Western blot (WB) analysis of whole-brain homogenate after proteinase K (PK) digestion from independent symptomatic (lines 2 to 9) and asymptomatic (lines 10 to 13) scrapie affected sheep. A molecular weight marker is loaded in lane 1. (B) Quantification of the WB signal of the PrPSc present in the brain homogenates is represented as PrP optical density (OD) signals. Our results indicate that the higher average amount of PrPSc was detected in the symptomatic scrapie affected sheep. The brain homogenate samples were normalized in relation to the total protein amount.
194x112mm (300 x 300 DPI)